

## Chemical sensors based on randomly stacked graphene flakes

Amin Salehi-Khojin,<sup>1,7,a)</sup> David Estrada,<sup>2,3</sup> Kevin Y. Lin,<sup>1</sup> Ke Ran,<sup>4,5</sup> Richard T. Haasch,<sup>5</sup> Jian-Min Zuo,<sup>4,5</sup> Eric Pop,<sup>2,3,6</sup> and Richard I. Masel<sup>7,a)</sup>

<sup>1</sup>Department of Chemical and Biomolecular Engineering, University of Illinois at Urbana-Champaign, Urbana, Illinois 61801, USA

<sup>2</sup>Department of Electrical and Computer Engineering, University of Illinois at Urbana-Champaign, Urbana, Illinois 61801, USA

<sup>3</sup>Micro and Nanotechnology Lab, University of Illinois at Urbana-Champaign, Urbana, Illinois 61801, USA

<sup>4</sup>Department of Material Science and Engineering, University of Illinois at Urbana-Champaign, Urbana, Illinois 61801, USA

<sup>5</sup>Materials Research Laboratory, University of Illinois at Urbana-Champaign, Urbana, Illinois 61801, USA

<sup>6</sup>Beckman Institute, University of Illinois at Urbana-Champaign, Urbana, Illinois 61801, USA

<sup>7</sup>Dioxide Materials, 60 Hazelwood Dr., Champaign, Illinois 61820, USA

(Received 8 November 2011; accepted 21 December 2011; published online 18 January 2012)

We demonstrate a simple fabrication method to produce randomly stacked graphene chemiresistors using surfactant-assisted exfoliation of graphite. We analyze the sensitivity of such chemiresistors as a function of vacuum filtration volume and temperature. At low vacuum filtration volumes ( $< \sim 5$  mL) the sensors exhibit superior sensitivity towards target molecules compared to previously developed polycrystalline graphene, polycrystalline graphene microribbon, and carbon nanotube chemical sensors. Temperature dependent measurements, transmission electron microscopy and scanning electron microscopy suggest the improved sensitivity in the randomly stacked graphene chemiresistors is due to 2-dimensional charge carrier hopping through edge defects. © 2012 American Institute of Physics. [doi:10.1063/1.3676276]

Graphene is an atomically thin sheet of covalently bonded carbon atoms arranged in a honeycomb crystal lattice. Its delocalized  $\pi$  bonds give rise to unique electronic properties<sup>1</sup> which are easily influenced by the environment due to fully exposed surface area and lack of bulk volume. Graphene has demonstrated significant potential as a material for chemical sensing because its 2-dimensional structure results in a high sensing area per unit volume, and because it exhibits low  $1/f$  noise compared to other solid state sensors.<sup>2</sup> Previous efforts have reported graphene sensors made via mechanical exfoliation,<sup>3</sup> epitaxial growth,<sup>4</sup> chemical vapor deposition,<sup>5</sup> and reduction of graphene oxide.<sup>2</sup> However, there have been no reports on graphene sensors made from surfactant/solvent exfoliated graphene (SEG). SEG (Refs. 6 and 7) does not require high temperatures or harsh chemical reducing agents during processing.

The objective of this work is to explore the chemical sensitivity of chemiresistors produced from SEG. We use sodium cholate surfactant for exfoliating graphene flakes in solution. Graphite flakes (1.5 g) are dispersed in 0.5% weight/volume (w/v) sodium cholate in Millipore water (100 ml). Sixty minutes of low-powered ultrasonication are performed to exfoliate graphite to graphene. After 90-min centrifugation (at 500 rpm), the top 80% of supernatant is decanted and retained for use. We then use vacuum filtration to create a randomly stacked graphene film, and through a stamp printing technique, deposit the film onto predefined gold electrodes on SiO<sub>2</sub>/Si substrates to form the chemiresistors. We perform experiments to determine (1) how charge transport occurs in randomly stacked SEG films, which form an electronically and structurally inhomogeneous system (overlap-

ping graphene islands) and (2) how this affects the sensitivity of graphene chemiresistors when they are exposed to different analyte molecules.

Figures 1(a) and 1(b) show an optical image and schematic cross section, respectively, of a typical sensor used in this study. Figures 1(c)–1(e) show scanning electron microscopy (SEM) images of the graphene film at different filtration volumes (3, 5, 10 ml, respectively). The SEM images reveal that the films progress from sparsely distributed to dense as the filtration volume increases. Figure 1(f) shows the Raman spectrum of the graphene film at 3 ml filtration volume. The significant presence of the Raman D band suggests defects in the graphene films, most likely from point defects and the edges of individual graphene islands, which can break the in-plane symmetry of the lattice vibrations.<sup>8</sup>

We characterize the conduction and sensing nature of SEG films vs. filtration volume in Figure 2(a). We note that the conductance of the film can be controlled across 5 orders of magnitude simply by controlling the filtration volume between 2 and 6 ml. However, the conductance increases only by another order of magnitude when the filtration volume is increased from 6 up to 10 ml. The 6 order of magnitude difference, ranging from  $10^{-8}$  to  $10^{-2}$  S between the thinnest and thickest films, highlights the possibility of tuning the chemical sensitivity of the graphene films by controlling the film density. The devices in this work showed repeatable performance with negligible standard deviation as seen in Figure 2(a). Five different sensors have been used for each filtration volume chosen from different graphene batches for the conductance and sensing experiments. We also observed that the  $1/f$  noise level increases by around 50× between thinnest and thickest films.<sup>9</sup>

We compared the conductance trend with the standard percolation theory described by  $\sigma \sim (N - N_c)^z$ , where  $\sigma$  is the

<sup>a)</sup>Authors to whom correspondence should be addressed. Electronic addresses: salehikh@illinois.edu and rich.masel@dioxidematerials.com.

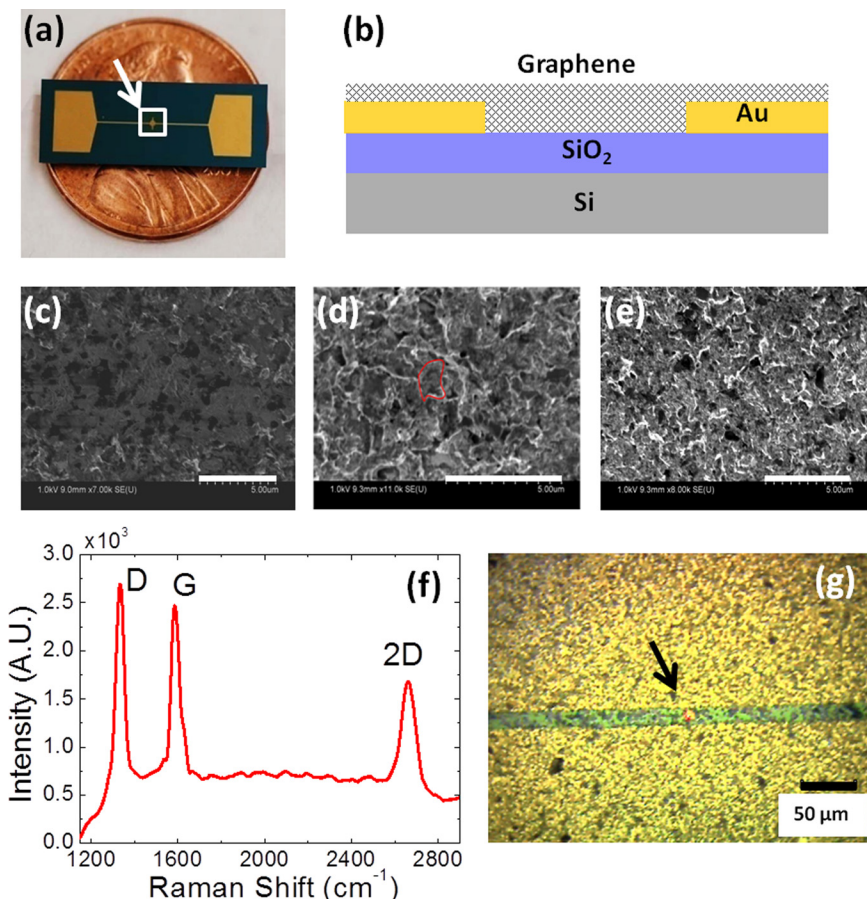


FIG. 1. (Color online) (a) Optical image of graphene sensor. Graphene films span the  $\approx 6 \mu\text{m}$  gap between the electrodes within the boxed region (magnified in (g)), (b) schematic cross section of the sensor, (c)-(e) SEM images of the randomly stacked graphene sensors obtained with 3, 5, and 10 ml filtration volumes, respectively. Scale bars are  $5 \mu\text{m}$ , and the red close contour in (d) outlines a typical flake, (f) Raman spectrum of the 3 ml sensor, and (g) magnified optical image taken with the boxed region of (a) with arrow indicating the location where Raman spectrum was collected.

conductance,  $N$  is the volume concentration of graphene solution,  $N_c$  is the critical volume concentration, and  $\alpha$  is a critical fitting exponent ( $\alpha \approx 1.94$  for 3-dimensional structures).<sup>10</sup> The best fit to the experimental data is shown in Figure 2 with

$\alpha = 1.77$ . However, the simple percolation theory does not follow the data at low filtration volumes. Rather, the experiments indicate two regions for the conductance, with higher and lower slopes as a function of filtration volume.

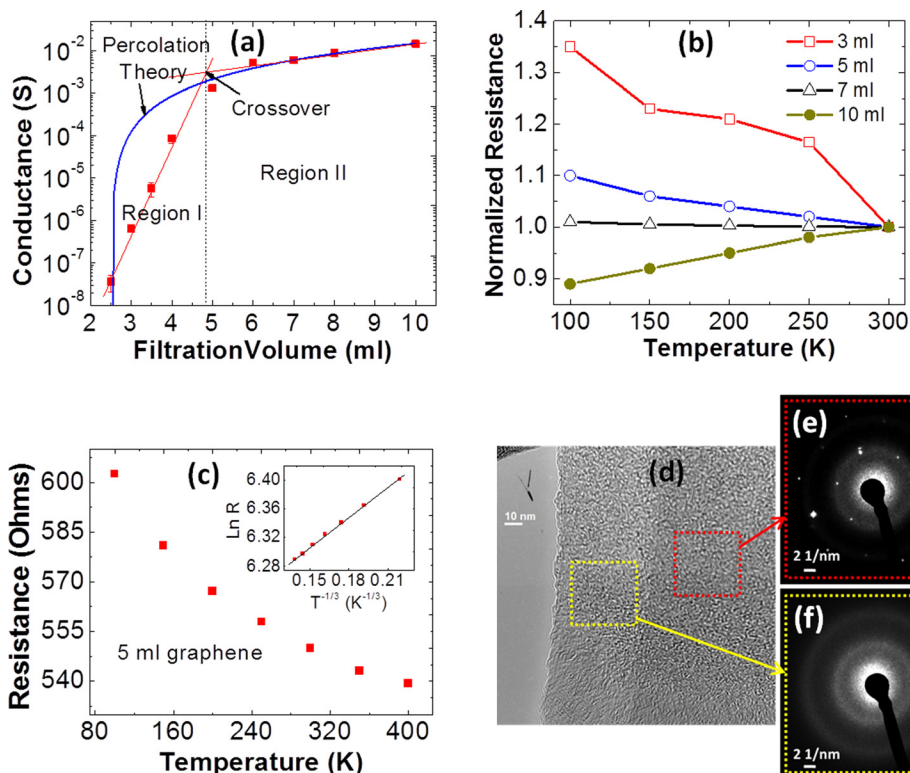


FIG. 2. (Color online) (a) Experimental (symbols) and theoretical (lines) conductance (S) vs. filtration volume (ml) for randomly stacked graphene sensors. (b) Resistance of different graphene sensor filtration volumes (normalized to value at room temperature) from 100-300 K, (c) temperature dependent resistance of the 5 ml graphene sensor from 100-400 K. The inset shows the linear fitting of  $\ln(R)$  to  $T^{-1/3}$  according to the Mott variable range hopping model, indicative of 2-dimensional electron hopping, (d) high resolution transmission electron microscopy (TEM) image of a representative graphene flake, (e) diffraction pattern in inner region of the flake showing the hexagonal structure of crystalline graphene (bright spots), and (f) diffraction pattern near the edge of flake showing characteristic rings due to the loss of long-range order (only weak and diffused diffraction intensity).

To elucidate the transport mechanisms of the two conductance regions, we performed temperature-dependent measurements. Figure 2(b) shows the resistance ( $R = 1/\sigma$ ) of the graphene sensors normalized to room temperature over the temperature range 100-300 K. At lower filtration volumes, the sensor resistance scales inversely with temperature, while at higher filtration volumes (around 10 ml) the resistance of the graphene film increases monotonically with temperature, suggesting metallic-like behavior. This is indicative of a transition in the electric transport regime from thermally assisted hopping to phonon limited conduction as the thickness of the film increases.<sup>11,12</sup> At  $\sim 7$  ml filtration volume the resistance becomes independent of temperature, showing a domain where thermally assisted hopping and phonon-limited conduction have approximately an equal and opposite role. These results indicate that it is possible to control the electric transport mechanisms in such SEG films, from semiconducting-like to metallic-like, simply by engineering the film density through the filtration volume. Such control has not been previously reported for SEG films over such a broad temperature range.

We gain further insight into the thermally-assisted transport mechanism of the semiconducting-like SEG films through closer examination of the resistance in the temperature range 100-400 K (Figure 2(c)). We use the Mott variable range hopping (VRH) model to fit the data of a representative sensor ( $\sim 5$  ml filtration volume) near the crossover point labeled in Figure 2(a)

$$R(T) = R_0 \exp[-(T_0/T)^{1/(n+1)}],$$

where  $R_0$  is a constant,  $T_0$  is the characteristic temperature, and  $n$  is the dimensionality of electron hopping. We find the electric transport within the randomly stacked SEG films at this concentration is determined by a 2-dimensional electron hopping mechanism,  $n=2$ . This is illustrated in the inset of Figure 2(c), where we find a linear fit to  $\ln(R)$  versus  $T^{-1/3}$  for the 5 ml sensor. Similar results were obtained for sensors with 3.5 and 4 ml volume filtration.

To gain additional insight into electrical transport through the morphology of our SEG samples, we used transmission electron microscopy (TEM) using a JEOL 2200FS TEM operated at 80 kV.<sup>13</sup> This voltage is below the knock-on damage threshold of the C-C  $sp^2$  bond and will not change the fully bonded graphene structure.<sup>14</sup> Figure 2(d) shows the high resolution image of a graphene flake under TEM. Diffraction patterns were obtained for both the edge and inner region of the sample, as highlighted by the boxed regions. The upper right pattern (Figure 2(e)) reflects the hexagonal structure of pristine graphene<sup>13,15</sup> while the lower right pattern (Figure 2(f)) corresponds to an amorphous structure. TEM results indicate that our individual graphene islands are heterogeneous systems with an inner region of ordered carbon atoms but with disordered edges. The disordered regions may arise from a combination of residual molecules from processing, build up during high resolution electron imaging and possible high edge defect populations on the graphene islands as previously reported.<sup>6,16</sup> SEM showed that at our lowest concentrations (3 ml filtration volume) the SEG film is sparsely distributed on the surface with

little coverage (Figure 1(c)). Thus, there are fewer connected paths for electron hopping, and less overlap between the pristine regions of the individual graphene flakes, resulting in large barriers for electron transport and 2-dimensional electron hopping. As a result, the conductance of the film is lower. SEM also shows that thicker graphene films (i.e., 10 ml filtration volume), are densely packed with almost complete coverage on the surface (Figure 1(e)). The higher density yields more paths for electrons to travel, with an increased overlap of the graphene islands' pristine areas, which reduces the overall disorder of the films and the barriers to transport.

We performed experiments to analyze the sensitivity of the randomly stacked SEG sensors with varying concentrations to 100 ms pulses of toluene (an electron donor) and 1,2-dichlorobenzene<sup>9</sup> (an electron acceptor). In each case, we chose the number of molecules in the pulse to be similar to the number of molecules produced by our preconcentrator with sampling air containing 300 parts-per-billion (ppb) of analyte. Figure 3(a) shows the sensitivity percent change to toluene for SEG chemiresistors obtained at graphene filtration volumes from 3 to 10 ml. The sensitivity is defined as  $(R-R_0)/R_0$ , where  $R_0$  is the initial resistance of the sensor in a background of ultrahigh purity helium gas and  $R$  is the resistance after exposure to the target analyte molecules. We note the sensitivity of the SEG films decreases with increasing graphene filtration volumes. The sensitivity is highest at  $\sim 14\%$  for the 3 ml filtration volume, and lowest at  $\sim 1.5\%$  for the 10 ml filtration volume.

Figure 3(b) compares the sensing responses to toluene of chemiresistors ranging from randomly stacked SEG sensors to previously developed polycrystalline (CVD) graphene, polycrystalline (CVD) graphene microribbons, and carbon nanotube (CNT)<sup>17</sup> sensors under the same experimental conditions. For polycrystalline graphene, the maximum response is  $\sim 2.5\%$  which corresponds to SEG filtration volume above 7 ml. For highly defective CNT sensors, the maximum response is  $\sim 4.2\%$  which is approximately that of the 6 ml filtration volume SEG sensors. Polycrystalline graphene microribbon sensors exhibit  $\sim 5.5\%$  maximum response, which corresponds to 5 ml SEG filtration volume. Below 4 ml SEG filtration volume, the randomly stacked SEG sensors show superior sensitivity as compared to all other types.<sup>17</sup>

Figure 3(c) compares the sensing responses to 1,2-dichlorobenzene molecules. Below 3.5 ml filtration volume the randomly stacked SEG sensors show similar sensing as polycrystalline graphene microribbon sensors. For polycrystalline graphene, the maximum response is at 6%, which corresponds to graphene filtration volume at 4 ml. For highly defective CNT sensors,<sup>17,18</sup> the maximum response is at 3.5%, which is approximately the response for randomly stacked SEG sensors in the range of 5 to 10 ml filtration volume. These results indicate that randomly stacked SEG sensors exhibit superior sensitivity to analyte molecules than other types of graphene and CNT sensors.

We believe the increased sensitivity of SEG chemiresistors occurs because the sodium cholate assisted exfoliation produces islands of graphene with an inner region of well-ordered carbon atoms surrounded by outer regions of disorder near the edges of the islands.<sup>11</sup> This arrangement produces

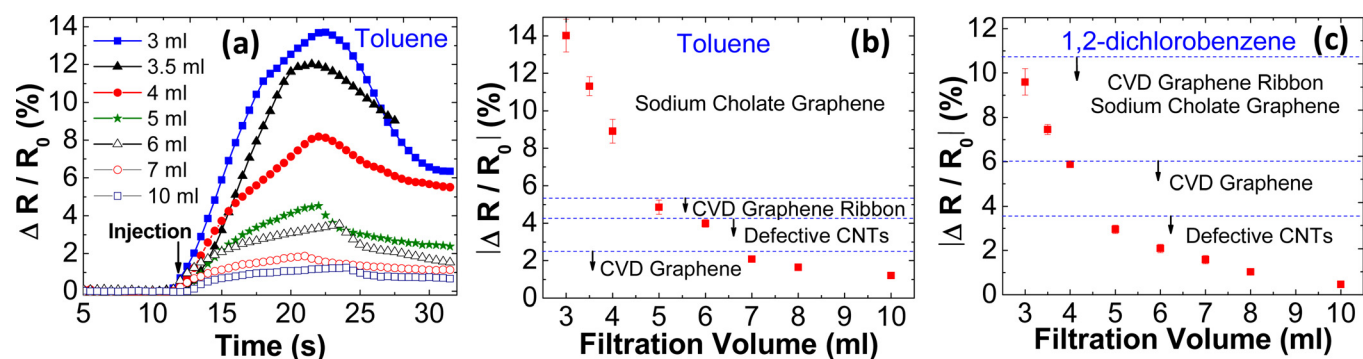


FIG. 3. (Color online) (a) Sensitivity response (%) of randomly stacked SEG sensors with varying filtration volumes to 100 ms pulse of  $10^{14}$  toluene molecules. (b) Maximum sensitivity response of SEG sensors vs. graphene filtration volumes from (a). The dashed lines represent maximum responses from polycrystalline (CVD) graphene, polycrystalline (CVD) graphene microribbons, and highly defective CNT sensors to the same dosage of toluene (Ref. 17). (c) Sensitivity response of SEG sensors vs. graphene filtration volumes to 100 millisecond pulse of  $10^{14}$  1,2-dichlorobenzene molecules (Ref. 9). The dashed lines represent maximum responses from polycrystalline (CVD) graphene, polycrystalline (CVD) graphene microribbons, and highly defective CNT sensors to same dosage of 1,2-dichlorobenzene.

closed contour defects, which could be more efficient than point and line defects for chemical sensing when operated in the electron hopping regime. Therefore it is not surprising to see the superior sensitivity observed from thinner graphene films (<5 ml filtration volume) compared to polycrystalline graphene, graphene microribbon, and defective CNT sensors. However, as the graphene film thickness increases (filtration volume increases), the electric transport transition occurs from 2-dimensional electron hopping to phonon limited (metallic) conduction, which is less efficient for chemical sensing.<sup>18</sup> This transition is one possible explanation for the drop in sensitivity with increasing filtration volume.

In summary, we developed simple chemiresistors with randomly stacked graphene films using surfactant-assisted exfoliation of graphite and tested for target analyte molecule sensitivity. It was shown that at low filtration volumes, the sensors showed superior sensitivity towards target molecules compared to previously developed polycrystalline graphene, polycrystalline graphene microribbon, and CNT chemical sensors. We observed that as the graphene film thickness increases, there is a shift in the electric transport regime from 2-dimensional electron hopping to phonon-limited (metallic) conduction, which explains the drop in sensitivity as the filtration volume increases.

This work was supported by National Science Foundation IIP-1046384, Office of Naval Research N00014-10-1-0853, and Dioxide Materials Company. D.E. and K.Y.L. contributed equally to this work. D.E. acknowledges support from the NSF and NDSEG Graduate Fellowship Programs. We would like to thank Albert Liao and Chris Neumann for help with 1/f noise measurements of SEG sensors.

<sup>1</sup>A. K. Geim and K. S. Novoselov, *Nat. Mater.* **6**(3), 183 (2007); K. S. Novoselov, A. K. Geim, S. V. Morozov, D. Jiang, M. I. Katsnelson, I. V. Grigorieva, S. V. Dubonos, and A. A. Firsov, *Nature* **438**(7065), 197 (2005).

<sup>2</sup>J. T. Robinson, F. K. Perkins, E. S. Snow, Z. Wei, and P. E. Sheehan, *Nano Lett.* **8**(10), 3137 (2008).

<sup>3</sup>Y. Dan, Y. Lu, N. J. Kybert, Z. Luo, and A. T. C. Johnson, *Nano Lett.* **9**(4), 1472 (2009); F. Schedin, A. K. Geim, S. V. Morozov, E. W. Hill, P. Blake, M. I. Katsnelson, and K. S. Novoselov, *Nat. Mater.* **6**(9), 652 (2007).

<sup>4</sup>R. Pearce, T. Iakimov, M. Andersson, L. Hultman, A. L. Spetz, and R. Yakimova, *Sens. Actuators B* **155**(2), 451 (2011).

<sup>5</sup>R. K. Joshi, H. Gomez, F. Alvi, and A. Kumar, *J. Phys. Chem. C* **114**(14), 6610 (2010).

<sup>6</sup>S. De, P. J. King, M. Lotya, A. O'Neill, E. M. Doherty, Y. Hernandez, G. S. Duesberg, and J. N. Coleman, *Small* **6**(3), 458 (2010).

<sup>7</sup>M. Lotya, Y. Hernandez, P. J. King, R. J. Smith, V. Nicolosi, L. S. Karlsson, F. M. Blighe, S. De, W. Zhiming, I. T. McGovern, G. S. Duesberg, and J. N. Coleman, *J. Am. Chem. Soc.* **131**(10), 3611 (2009); A. B. Bourlinos, V. Georgakilas, R. Zboril, T. A. Sterioti, and A. K. Stubos, *Small* **5**(16), 1841 (2009).

<sup>8</sup>L. G. Cancado, K. Takai, T. Enoki, M. Endo, Y. A. Kim, H. Mizusaki, A. Jorio, L. N. Coelho, R. Magalhaes-Paniago, and M. A. Pimenta, *Appl. Phys. Lett.* **88**(16), 163106 (2006); A. Jorio, M. Dresselhaus, R. Saito, and G. F. Dresselhaus, *Raman Spectroscopy in Graphene Related Systems* (Wiley-VCH, Weinheim, Germany, 2011).

<sup>9</sup>See supplementary material at <http://dx.doi.org/10.1063/1.3676276> for 1/f noise measurements, XPS analysis, and sensor response to 1,2-dichlorobenzene.

<sup>10</sup>D. Stauffer and A. Aharony, *Introduction to Percolation Theory* (Taylor and Francis, Philadelphia, 1994).

<sup>11</sup>A. B. Kaiser, G. N. Cristina, R. S. Sundaram, M. Burghard, and K. Kern, *Nano Lett.* **9**(5), 1787 (2009).

<sup>12</sup>A. B. Kaiser and V. Skakalova, *Chem. Soc. Rev.* **40**(7), 3786 (2011).

<sup>13</sup>J. Zhang, J. Xiao, X. Meng, C. Monroe, Y. Huang, and J.-M. Zuo, *Phys. Rev. Lett.* **104**(16), 166805 (2010).

<sup>14</sup>L. W. Hobbs, *Ultramicroscopy* **23**(3-4), 339 (1987).

<sup>15</sup>Y. Hernandez, V. Nicolosi, M. Lotya, F. M. Blighe, Z. Sun, S. De, I. T. McGovern, B. Holland, M. Byrne, Y. K. Gun'Ko *et al.*, *Nat. Nanotechnol.* **3**(9), 563 (2008).

<sup>16</sup>J. M. Englert, C. Dotzer, G. Yang, M. Schmid, C. Papp, J. M. Gottfried, H.-P. Steinrück, E. Spiecker, F. Hauke, and A. Hirsch, *Nat. Chem.* **3**(4), 279 (2011).

<sup>17</sup>A. Salehi-Khojin, D. Estrada, K. Y. Lin, M. Bae, F. Xiong, E. Pop, and R. I. Masel, *Adv. Mater.* **24**(1), 53 (2012); A. Salehi-Khojin, K. Y. Lin, C. R. Field, and R. I. Masel, *Science* **329**(5997), 1327 (2010).

<sup>18</sup>A. Salehi-Khojin, F. Khalili-Araghi, M. A. Kuroda, K. Y. Lin, J. P. Leburton, and R. I. Masel, *ACS Nano* **5**(1), 153 (2010).